

NEW PHOSPHORUS COMPOUNDS $K[PCl_3(X)]$ ($X = SCN, CN$): PREPARATION AND DFT AND SPECTROSCOPIC STUDIES

AMIR LASHGARI^a, SHAHRIAR GHAMAMI^a GUILLERMO SALGADO-MORAN^b, RODRIGO RAMIREZ-TAGLE^c AND LORENA GERLI – CANDIA^{d*}.

^a Department of Chemistry, Faculty of Science, Imam Khomeini International University, Qazvin,

^b Facultad de Ciencias Exactas, Departamento de Química, Universidad Andrés Bello, sede Concepción, Concepción, Chile.

^c Universidad Bernardo O'Higgins, Laboratorio de Bionanotecnología, General Gana 1780, Santiago, Chile.

^{d*} Universidad Católica de la Santísima Concepción, Facultad de Ciencias, Departamento de Química Ambiental, Concepción, Chile.

ABSTRACT

Two new phosphorus complexes, potassium trichlorothiocyanophosphate (III) (PTCTCP; $K[PCl_3(SCN)]$) and potassium trichlorocyanophosphate (III) (PTCCP; $K[PCl_3(CN)]$) were synthesized from the reaction of KSCN and KCN, respectively, with PCl_3 . The chemical formulas and compositions of these compounds were determined by elemental analysis and spectroscopic methods, such as phosphorus-31 nuclear magnetic resonance (NMR) spectroscopy (^{31}P -NMR), Fourier transform infrared (FTIR) spectroscopy, ultraviolet-visible (UV-Vis) spectroscopy and mass spectrophotometry. All of the theoretical calculations and determinations of the properties of these compounds were performed as part of the Amsterdam Density Functional (ADF) program. Excitation energies were assessed using time-dependent perturbation density functional theory (TD-DFT). In addition, the molecular geometry was optimized and the frequencies and excitation energies were calculated using standard Slater-type orbital (STO) basis sets with triple-zeta quality double plus polarization functions (TZ2P) for all of the atoms. The assignment of the principal transitions and total densities of state (TDOS) for orbital analysis were performed using the GaussSum 2.2 program.

Keywords: Phosphorus compound, DFT, ADF, Spectroscopic Studies.

1. INTRODUCTION

Organophosphorus complexes were first synthesized almost 200 years ago using reactions between alcohols and phosphoric compounds such as phosphoric acid. Organophosphorus chemistry is the conforming field and discipline surrounding the reactivity of organophosphorus complexes and products derived from them¹⁻³. These compounds are degradable organic compounds containing carbon-phosphorus bonds, and because of this degradability, compounds in this class are primarily used for pest control as an alternative to chlorinated hydrocarbons, which are preserved in the environment. In addition, they have been used as chemical warfare nerve agents⁴. Phosphorus chemistry has been developing in recent years as one of the most important branches of science⁵⁻⁶.

Theoretical calculations of organophosphorus and phosphonium complexes have good attention between researchers in many years⁷⁻¹⁰. Theoretical chemistry can be defined by way of a mathematical explanation of chemistry, while computational chemistry is typically used when a mathematical method is adequately fine established. A profound considerate of marvel needs the use of theoretical calculations¹¹. Density functional theory (DFT) methods are frequently measured to be ab initio methods for defining the molecular electronic structure, while numerous of the most common functionals use parameters resultant from more complex calculations. DFT methods have been gradually applied to the study of the communication of complexes¹²⁻¹³.

In the present study, we synthesized and characterized novel organophosphorus compounds using Phosphorus-31 nuclear magnetic resonance (NMR) spectroscopy (^{31}P -NMR), Fourier transform infrared (FTIR), ultraviolet-visible (UV-Vis) spectroscopy and elemental analysis. In addition, we used theoretical studies to determine more of the details and to peruse the data obtained. We observed an excellent correlation between our theoretical data and our experimental data, especially the spectroscopic results.

2. EXPERIMENTAL

2.1. Materials and Instruments

All of the materials used in this study (KSCN, KCN, PCl_3 , and hexane (99%)) were purchased from Merck & Co., Inc. The solvents that were used in the reactions were purified and dried following standard procedures. Infrared spectra were recorded as KBr disks using a Bruker Tensor model 420 spectrophotometer. Mass spectra were recorded using an Agilent Technology (HP) Network Mass Selective Detector 5973 spectrophotometer. The UV-Vis spectra were recorded using a Camspec WPA Biowave 350 spectrophotometer. So, ^{31}P -NMR information was obtained by using NMR 500 MHz model BRUKER AVANCE DRX 500 in DMSO solvent.

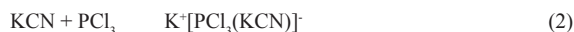
2.2. The Synthesis of PTCTCP

Potassium trichlorothiocyanophosphate (III) (PTCTCP) was prepared by dissolving powdered KSCN (0.2 g; 2.06 mmol) in PCl_3 (0.18 ml) and stirring for 4 h at room temperature while maintaining a 1:1 KSCN: PCl_3 ratio. This product could be easily prepared with a good yield by combining potassium thiocyanate with phosphorus trichloride using equation (1). Stirring was continued until a pink sediment was formed. The sediment mixture was then washed with hexane and dried. The results of analyzing the sediment were as follows: FTIR (KBr) (cm^{-1}): 459.67 (ν_{P-Cl}), 537.67 (ν_{P-S}), 1131.74 (ν_{C-N}), 2063.56 (ν_{SCN}), 1589.24 ($\nu_{C=N}$) cm^{-1} ; ^{31}P NMR (135 MHz, $CDCl_3$): $\delta = 1.49$ ppm; UV-Vis in CH_3CN , λ/cm^{-1} : 240, 280, 305, 360; Mass: M/e = 159, 101.



2.3. The Synthesis of PTCCP

Potassium trichlorocyanophosphate (III) (PTCCP) was prepared by dissolving ground KCN (0.16 g, 2.45 mmol) in PCl_3 (0.16 ml) and stirring for 4 h at room temperature while maintaining a 1:1 KCN: PCl_3 ratio (2). The stirring was constant until a product was formed, and then, the mixture was filtered, resulting in a blue sediment solution. Finally, the sediment mixture was washed with hexane and dried. The results of analyzing the sediment were as follows: FTIR (KBr) (cm^{-1}): 415.97 and 585.24 (ν_{P-Cl}), 1223.97 (ν_{P-C}), 1627.29 ($\nu_{C=N}$), 2100.72 ($\nu_{C=N}$) cm^{-1} ; ^{31}P NMR (135 MHz, $CDCl_3$): $\delta = 0.62$ ppm; UV-Vis in CH_3CN , λ/cm^{-1} : 225, 340; Mass: M/e = 173, 198.



2.4. Calculation methods

Our molecular calculations were performed using the Amsterdam Density Functional (ADF) code¹⁴. The scalar relativistic effects were incorporated by using the zero-order regular approximation (ZORA)¹⁴⁻¹⁶. All of the molecular structures were fully optimized via the analytical energy gradient method implemented by Verluis and Ziegler that employs the local density approximation (LDA) within the Vosko–Wilk–Nusair parameterization for local exchange correlations¹⁷⁻¹⁸. We also used the GGA (generalized gradient approximation) SAOP (statistical average of orbital model exchange-correlation potential) functional¹⁹ which was specially designed for calculating optical properties. The excitation energies were estimated using a time-dependent perturbation density functional theory (TD-DFT)^{20,21}. The solvation effects were modeled using a conductor-like screening model for real solvents (COSMO)^{22,23} with acetonitrile as the solvent. Each excited state was introduced by a Gaussian output with a full width at half-maximum (fwhm) of 3000 cm^{-1} . The orbital contribution and the total density of state (TDOS) used in the orbital analysis

were analyzed using the GaussSum 2.2 software package²⁴. The TDOS was determined by convolving the molecular orbital (MO) data with Gaussian curves of unit height and a full width at half-maximum (fwhm) of 0.3 eV.

The optimal molecular geometry, frequencies and excitation energies were calculated using standard Slater-type orbital (STO) basis sets with triple-zeta quality double plus polarization functions (TZ2P) for all of the atoms²⁵.

3. RESULTS AND DISCUSSION

3.1. Structural properties of the molecular geometry

The structures of the optimized PTCTCP and PTCCP are shown in Figure 1. All of the ab initio calculations were made using the Amsterdam Density Functional (ADF) code¹⁴. The scalar relativistic effects were incorporated using the zero-order regular approximation (ZORA)¹⁴⁻¹⁶, and the calculated geometrical parameters for the compounds are shown in Table 1. This table shows the experimental values for the bond lengths and the mentioned references. For PTCTCP and PTCCP, the optimized C≡N bond lengths were both found to be 1.17 Å, which is close to the value reported by Allen et al.²⁶. For the thiocyanate bond with the phosphorous atom in PTCCP, the P-S and S-C bond lengths were 2.23 and 1.68 Å, respectively. These values are in agreement with the values reported by Okuniewski et al. for the P-S bond²⁷ and Rindorf et al. and Kenneth et al. for the S-C bond²⁸⁻²⁹. The P-C bond length in PTCCP was 1.82 Å; and this value was reported to be 1.92 and 1.81 Å by Athanassios et al. and Priya et al., respectively³⁰⁻³¹. The P-Cl bond lengths in both compounds have values between 2.1 and 2.68 Å, and Burck et al. reported a value of 2.33 Å³². These differences between bond lengths represent an electronegative effect caused by the cyano, thiociano and three-color groups.

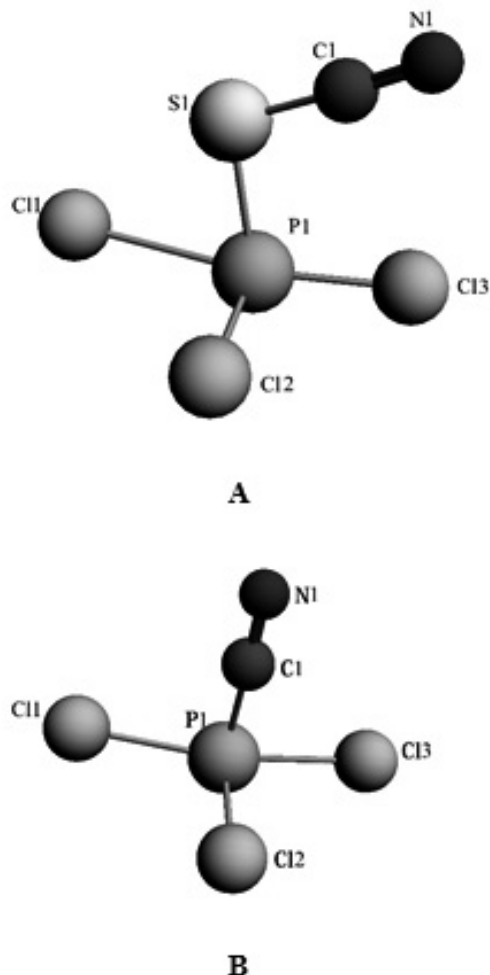


Figure 1. The optimized molecular structure of A) PTCTCP and B) PTCCP compounds.

By comparing the two phosphorous compounds, we found the following properties: a) various molecular radii and volumes that cause relative differences; b) miscellaneous dynamic rotations and inversions in two molecules; c) differences in the CN bond angle that can be used for secondary reactions. Molecular ions are commonly assumed to be in a hypothetical gaseous free state and without any pre-assumed symmetry. After the optimization procedures, which included creating a minimum-energy geometry, the vibrational frequencies and intensity spectra were calculated. The resulting structures of these compounds showed a difference in the π -donor ability of the CN and SCN ligands that was caused by the bending and distortion of the bond angles in the two compounds. The CN ligand has good π -donority due to the π -back bonding ability of this type of ligand, and can cause P-C-N angles to become linear, which was confirmed by our data (174.21).

In the $KPCl_3(SCN)$, the ADF and experimental data reported by Strasser et al.³³ showed bending and torsion in P-S-C at 104.12 and 104.48 degree angles, respectively. Therefore, for the rest of angles, the values are provided with values from references³⁴⁻³⁷ in Table 1. We have found a very good correlation between the calculated and experimental results. This difference in behavior can cause poisoning by attacking biological phosphorous acceptors and enzymes such as acetylcholine esterase. These types of studies can be used for simulations and theoretical studies of poisonous organophosphorous compounds. The eigenvectors of the normal models were calculated and displayed on a computer to identify the dominant motions. All of the theoretical results for the PTCTCP and PTCCP compounds correlated well with our experimental data³⁸⁻³⁹.

Table 1: Calculated geometrical parameters.

Bond	Bond length [Experimental] (Å)	Bond	Bond Angle (°)
PTCTCP			
C1-N1	1.17 [1.14] ^a	S1-P1-Cl1	74.04
S1-C1	1.68[1.64] ^e	S1-P1-Cl2	101.88[113.42] ^g
P1-S1	2.23[1.98] ^b	S1-P1-Cl3	99.81[110.9]G
P1-Cl1	2.68[2.33] ^d	C1-S1-P1	104.12[104.48] ^f
P1-Cl2	2.1	S1-C1-N1	176.66[178.3] ⁱ
P1-Cl3	2.18	Cl1-P1-Cl2	91.95
		Cl1-P1-Cl3	170.30
		Cl2-P1-Cl3	96.72[101.44] ^h
PTCCP			
C1-N1	1.17[1.14] ^a	N1-C1-P1	174.21
P1-C1	1.816[1.81] ^c	C1-P1-Cl1	86.03
P1-Cl1	2.39	C1-P1-Cl2	97.55
P1-Cl2	2.1	C1-P1-Cl3	86.03
P1-Cl3	2.39	Cl1-P1-Cl2	93.42
		Cl1-P1-Cl3	170.13
		Cl2-P1-Cl3	93.42[101.44] ^k

^aRef[25], ^bRef[26], ^cRef[29,30], ^dRef[31], ^eRef[27, 28], ^fRef[32], ^gRef[33], ^hRef[34], ⁱRef[35], ^jRef[36]

3.2. Vibrational spectra

In the vibrational spectra of these compounds, all of the expected bands were seen. For PTCTCP, the most important of these bands is associated with tensile motion of the P-Cl and P-S bonds (at 459.67 and 537 cm^{-1} , respectively); therefore, for PTCCP, the frequencies 415.97, 585.24 (P-Cl) and 1223.97 (P-C) were especially significant. Selected vibrational spectra of both compounds are compared with theoretical data in Table 2.

Table 2: Selected FTIR results for PTCTCP and PTCCP.

ν (cm ⁻¹) [Calculated]	Assignment	Intensity	ν (cm ⁻¹) [Calculated]	Assignment	Intensity
PTCTCP			PTCCP		
460[460] [‡]	ν_{P-Cl}	(m)	416, 585 [416, 585]	ν_{P-Cl}	(s), (w)
538[540]	ν_{P-S}	(m)	1224[1224]	ν_{P-C}	(vw)
1132[1130]	ν_{C-N}	(vw)	1627[1628]	$\nu_{C=N}$	(vw)
2064[2064]	$\nu_{SC=N}$	(s)	2101[2101]	$\nu_{C=N}$	(vw)
1589[1590]	$\nu_{C=N}$	(w), (m)			

w: weak, vw: very weak, m: medium, s: strong

The frequencies (wave numbers) must be correlated with the results of FTIR spectroscopy. The calculated and experimental vibrational spectra correlated well⁴⁰⁻⁴¹. The calculated wave number (frequency) scale was often slightly too high due to the poor modelling of the orbitals and their interactions with the surroundings. The present contributions aim to build a collection of experimental data for the preparation of a novel phosphorus compound⁴². The pictures in Figure 1 show the similarity of the theoretical and experimental results. As shown, all of the calculated bands were present in the experimental data. Simple and mixed overtones and limitations in the resolution of experimental instruments made the experimental spectra broad and blurred.

showed the main signal at 1.49 and 0.62 ppm, respectively (Figure 2). This single resonance in the ³¹P-NMR spectrum demonstrated a phosphorus atom as a central ion. Chemical shift ³¹P is pretty broad, in fact diverse states in the phosphorus valence does not follow a predictable pattern. In the PTCTCP spectrum, the peak (1.49 ppm) was shown which represented a phosphorous chemical shift with the SCN ligand at higher field, while in the PTCCP spectrum this shift with the CN ligand occur at lower field around zero. By comparison of these chemical shifts with other phosphorous compounds, such as acidity forms, a shielding was made by CN and SCN electron change transferring to a phosphorous atom.

3.3. ³¹P-NMR

The experimental ³¹P-NMR spectrum of PTCTCP and PTCCP compounds

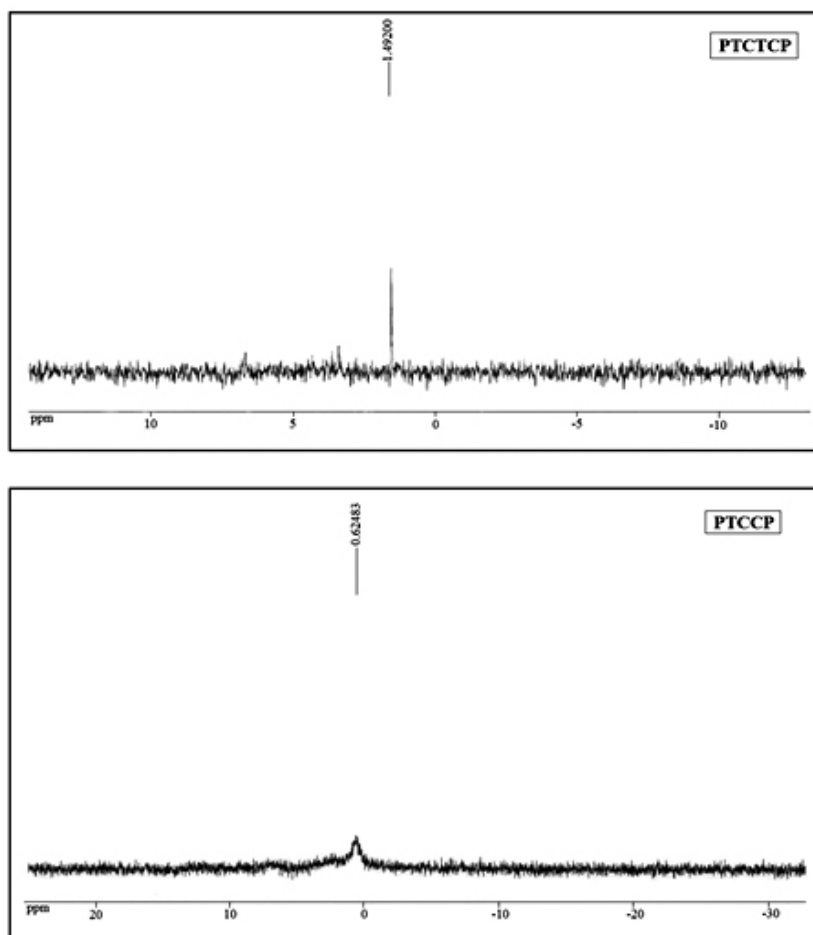


Figure 2. ³¹P-NMR spectra for PTCTCP and PTCCP complexes.

3.4. UV/Visible spectra

The calculated and experimental UV-Visible spectra showed very good conformation and correlation. Calculated peaks and transitions are found in experimental spectra, and if no peak appeared, it was because it overlapped with other peaks (as in the case of PTCCP). These data show how the spectra change according to the ligands or substitutes in these compounds. In the UV-Visible spectra of PTCTCP and PTCCP, the transitions were at 3 and 2, respectively, and their specifications, transition character and assignment of principal transitions are shown in Table 3.

Table 3: Experimental and calculated (TD-DFT) electronic absorption spectra in the visible range for PTCTCP and PTCCP.

Experiment λ/nm (ϵ)/ $\text{dm}^3\text{mol}^{-1}\text{cm}^{-1\text{a}}$	Theory λ/nm (f) ^b	Transition character	Assignment of principal transitions ^c
PTCTCP			
(1800) 240	260 (0.33)	$n \rightarrow \pi^*$ $A_1 \rightarrow A_1^*$	H-2 L (0.98)
	257 (0.07)		
	251 (0.02)		H L+1 (0.66) H-3 L (0.03)
	250 (0.07)		
(970) 280	281 (0.03)	$\pi \rightarrow \pi^*$ $A_1 \rightarrow E^*$	H-1 L (0.94)
	267 (0.01)		
305 (540)	299 (0.006)	$\pi \rightarrow \pi^*$ $A_1 \rightarrow E^*$	H L (0.96)
	286 (0.04)		
(120) 360	341 (0.06)	$n \rightarrow \pi^*$ $A_1 \rightarrow A_1^*$	
PTCCP			
225 (2100)	248 (0.01)	$\pi \rightarrow \pi^*$ $E \rightarrow A_1^*$	
	238 (0.05)		
	235 (0.05)		H-2 L (0.95)
	228 (0.27)		H-1 L (0.64) H L+1 (0.03)
340 (580)	344 (0.03)	$n \rightarrow \pi^*$ $A_1 \rightarrow A_1^*$	
	290 (0.16)		
	280 (0.16)		

^a Experimental data were recorded in acetonitrile solution unless stated otherwise.

^b Calculated absorptions in the solid phase were found using TD-DFT; the figures in parentheses indicate the oscillator strength.

^c The calculated transition assignments in parentheses indicate fractional contributions to the calculated absorptions.

First, the experimental value of λ for PTCTCP were 240, 280, 305 and 360 nm, which can be compared the calculated values of 260, 281, 299 and 341 nm, respectively, which are in very good agreement. This complex has $\pi \rightarrow \pi^*$ ($A_1 \rightarrow E^*$) (linked to charge transitions (CT)) and $n \rightarrow \pi^*$ ($A_1 \rightarrow A_1^*$) transition wavelengths of 280/305 and 340/360 nm, respectively. Because of inner transition of SCN, CN and the loss of symmetry from Td to C_{3v}, the intensity of the peaks was increased; this increase is associated with the shoulder at 305 nm (Figure 3).

Therefore, for the PTCCP compound, the two transfer characteristics listed in Table 3 have been identified. The combined transfer $n \rightarrow \pi^*$ ($A_1 \rightarrow A_1^*$) at a wavelength of (340 nm) $\pi \rightarrow \pi^*$ ($E \rightarrow A_1^*$) with a transmission wavelength of 225 nm are related to charge transfer. Figure 3 shows the UV spectra of both of these compounds. The high intensity transition spectra in experimental

(theoretical calculation) were at 240 (260) and 225 (228) nm for PTCTCP and PTCCP, respectively, which describes important absorption properties of both compounds. For PTCTCP, the experimentally observed absorption at 240 nm arises from excitations of HOMO-2 to LUMO, whereas, for PTCCP, the 225 nm wavelength is associated with the ascent from HOMO-1/HOMO to LUMO/LUMO+1⁴³.

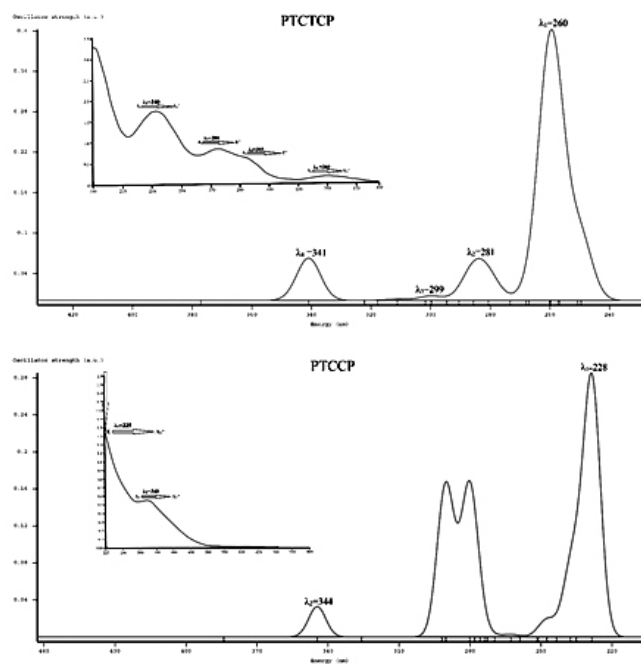


Figure 3. The experimental and calculated UV/Vis spectra of PTCCP and PTCTCP.

3.5. Frontier molecular orbitals

The HOMO represents the ability to donate an electron, and the LUMO is an electron acceptor. The electronic absorption corresponds to the transition from the ground to the first excited state and is generally described as the excitation of one electron in the highest occupied molecular orbital (HOMO) to the lowest unoccupied molecular orbital (LUMO)⁴⁴⁻⁴⁵.

The energies of the HOMO and the LUMO and their energy gap are evidence for the chemical activity of the molecules. Figure 4 shows the broadcast and energy levels of the HOMO-1, HOMO, LUMO and LUMO+1 and the energy gaps between excited and ground states for each compound. The energy gaps from the HOMO-1 to and the LUMO and the LUMO+1 of PTCTCP were (3.93, 4.60 eV) and from HOMO to LUMO and LUMO+1 were (4.31, 4.89 eV), respectively. For PTCCP, these energy gaps were (3.46, 4.13 eV) and (3.42, 4.00 eV), respectively. These energies and energy gaps indicate close energy states for both of the compounds. The TDOS of PTCTCP and PTCCP calculated with the GaussSum 2.2 program are shown in Figure 5. The TDOS plot shows the orbital population and validates a simple assessment of the character of the molecular orbitals⁴⁶⁻⁴⁷.

3.6. Mass spectra

The m/e: 159 and m/e: 198 in the mass spectra are the main reasons for synthesizing PTCTCP and PTCCP, respectively, and details for both compounds are shown in Figure 6. According to the isotopes, large peaks are visible, and the mass spectral characteristics of compounds are shown in Table 4. The intensities of the PTCTCP mass spectra are greater than those of PTCCP. In addition, m/e: 149, 42, 59, 60, 101/97, 112 are mainly high intensity peaks for PTCTCP/PTCCP, respectively. The resulting drop out species and expected species assignments are shown in Table 4.

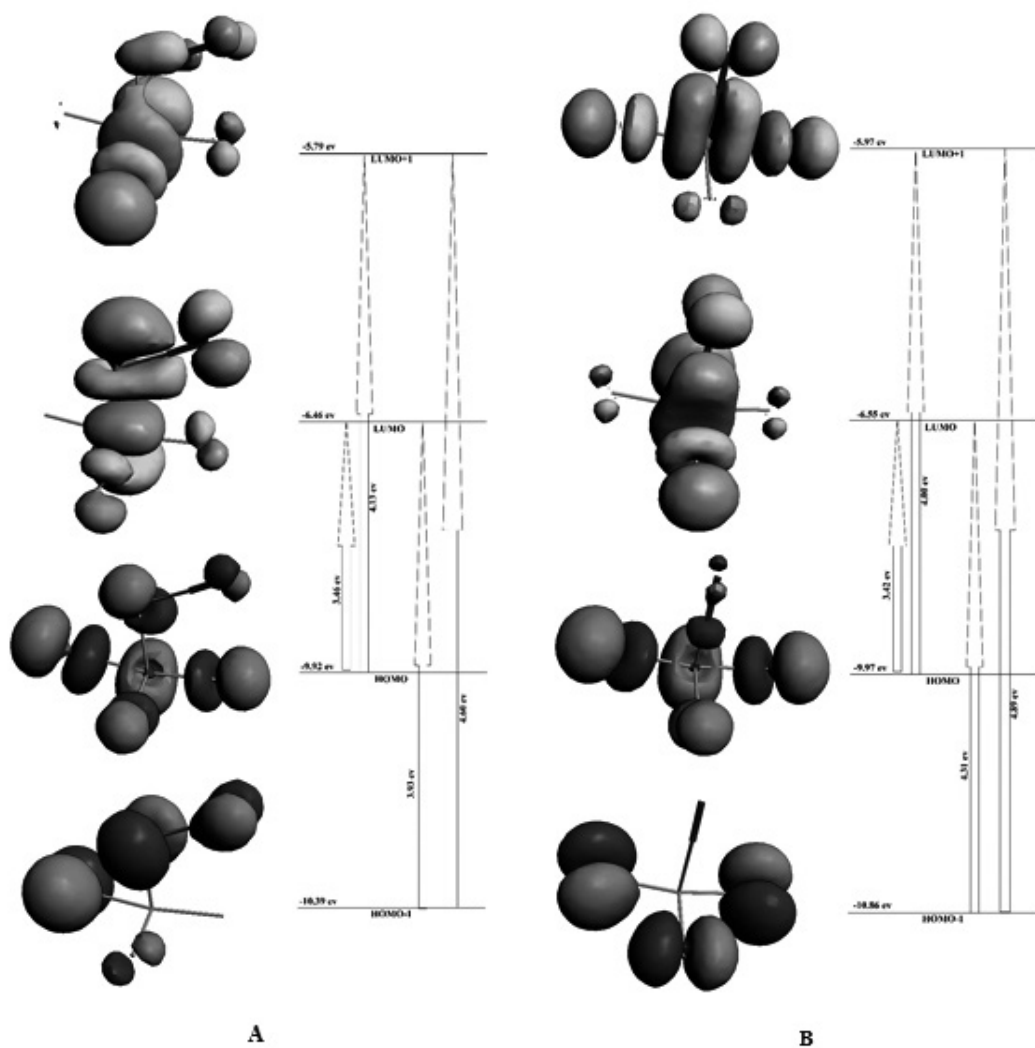


Figure 4. The frontier molecular orbitals of A) PTCTCP and B) PTCCP compounds.

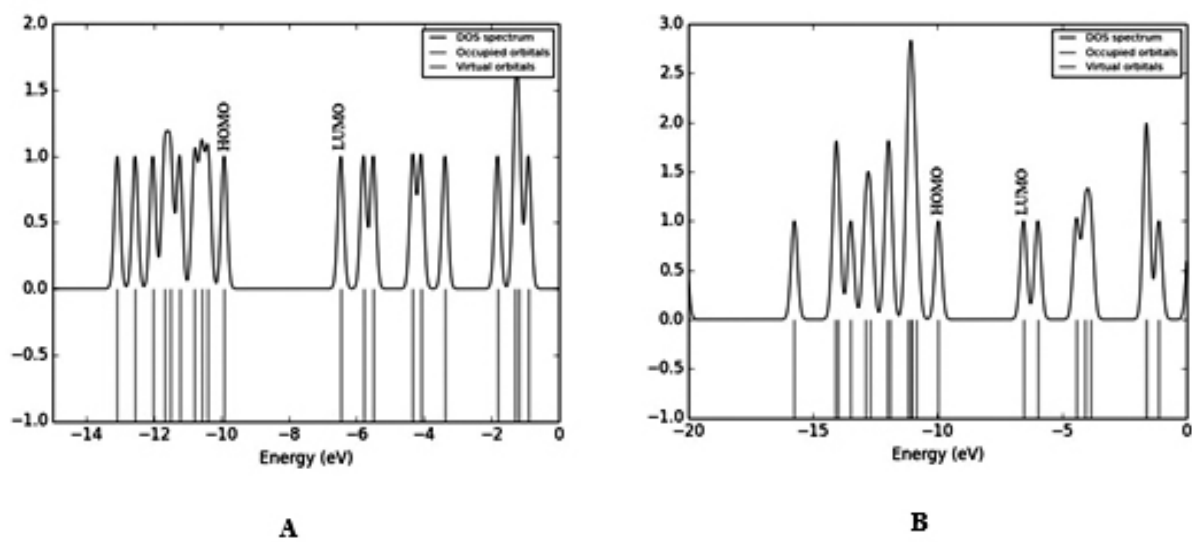


Figure 5. The total density of state (TDOS) graph for A) PTCTCP and B) PTCCP compounds.

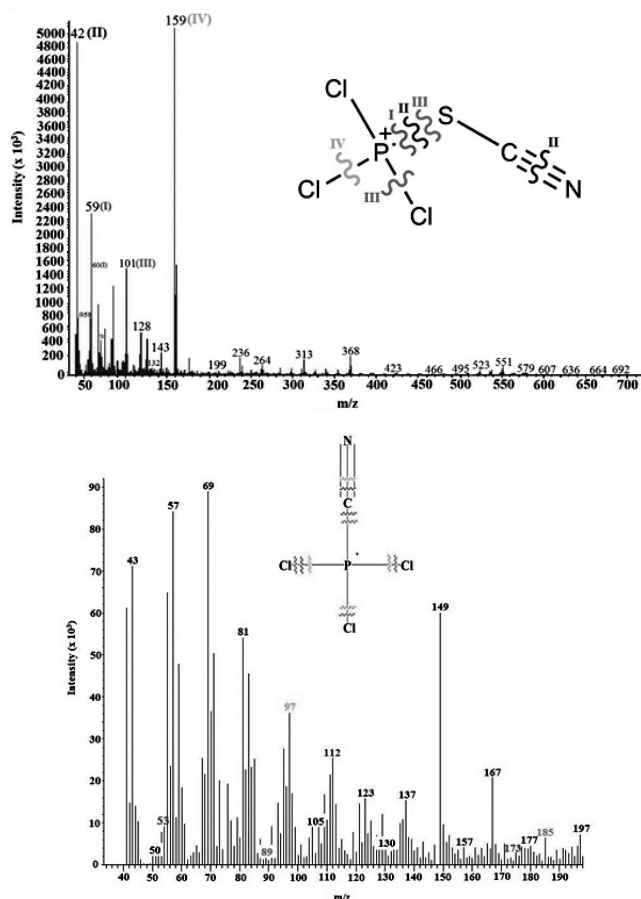


Figure 6. The experimental mass spectra.

Table 4: The mass spectrum characterization of PTCTCP and PTCCP.

Expected species	Drop out species	m/e	Intensity (x 10 ³)
PTCTCP			
[PCl ₂ SCN]	KCl	159	5040
[SC]	K[PCl ₃ N]	42	4850
[SCN]	K[PCl ₃]	59, 60, 58	2360, 1560, 840
[PCl ₂]	KSCN + KCl	101	1550
[PCl ₂ CN]	KS + KCl	128	412
[Cl ₃ S]	KPCN	143	280
[Cl ₃ CN]	KPS	132	90
PTCCP			
PCN	KCl ₃	53	7.826
PClCN	KCl ₂	89	1.585
Cl ₂ CN	KPCl	97	36.160
PCl ₂ N	KClC	112	25.528
KCl ₃ C	PN	157	4.194
KPCl ₃	CN ⁻	173	1.826
KPCl ₃ C	N ³⁻	185	6.443
KPCl ₃ CN	-	198	1.922
KP ₂ Cl ₆ CN	-	332	0.689

4. CONCLUSION

Potassium trichlorothiocyanophosphate (III) and potassium trichlorocyanophosphate (III) were synthesized from KSCN, KCN and PCl₃. Elemental analysis and spectroscopic devices were used to determine their chemical formulas and compositions. The eigenvectors for the normal models were calculated using a standard Slater-type orbital (STO) basis set with ADF software.

The geometrical parameters for each bond length agreed well with previously published data (REFERENCIA). By comparing these two phosphorous compounds, we found the following properties: a) various molecular radii and volumes that cause relative differences; b) miscellaneous dynamic rotations and inversions in the two molecules; c) different CN bond angles that can be used for secondary reactions.

Calculations using the wave number (frequency) scale are often slightly too high due to poor modelling of the orbitals and interactions with the surroundings. The present contribution aims to collect experimental data for the development of novel phosphorus compounds.

The experimental ³¹P NMR spectrum of the main signal of PTCTCP and PTCCP compounds were 1.49 and 0.62 ppm, respectively, showing that the complexes successfully synthesis and prepared.

The data from the UV-Vis spectra show how the spectra of these compounds depend on ligands or substitutes. The transitions of the PTCTCP and PTCCP compounds were at 4 and 2, respectively, and we described these experimental data and calculated their specifications, transition characters and assignment of principal transitions. The assignments of principal transitions and total density of state (TDOS) for the orbital analysis were calculated using the GaussSum 2.2 program. Closer energy states were indicated for frontier molecular orbitals (MOs) with energy gaps between the HOMO-1, HOMO, LUMO and LUMO+1 for both compounds.

In the mass spectra of PTCTCP and PTCCP, we detected major peaks at m/e: 159 and m/e: 198, respectively, which was the main reason for synthesizing these compounds.

REFERENCES

- Edmond R.T.; Organophosphorus Complexes of Cobalt Carbonyl as Hydroformylation Catalysts, *Ind. Eng. Chem. Prod. Res. Dev.*, 8 (3), 286–290, (1969).
- Jeffrey M.J.; Allen, W.V.; Lewis, W.C.; John, H.N.; Palladium(II) thiocyanate organophosphorus complexes, *Inorg. Chem.*, 19 (4), 1036–1039, (1980).
- Downing, J.H.; Smith, M.B. "Phosphorus Ligands". *Comprehensive Coordination Chemistry II*, 253–296, (2003).
- Balali-Mood, M.; Shariat, M. Treatment of organophosphate poisoning, Experience of nerve agents and acute pesticide poisoning on the effects of oximes. *J. Physiol Paris*, 92, 375 – 378, (1998).
- Quin, L. D.; *A Guide to Organophosphorus Chemistry*; John Wiley & Sons, (2000).
- Racke, K.D.; "Degradation of organophosphorus insecticides in environmental matrices", pp. 47–73 in: Chambers, J.E., Levi, P.E. (eds.), *Organophosphates: Chemistry, Fate, and Effects*. Academic Press, San Diego, (1992).
- Kabachnik, M. I.; Baranov, A. P.; Medved, T. Ya.; Theoretical conformational analysis of cyclopendant organophosphorus chelating agents, derivatives of cyclam, *Theoretical and Experimental Chemistry*, 26, 2, 169–174, (1990).
- Jenkins, J.M.; Verkade, J.G.; Stereochemistry of organophosphorus complexes of transition metals, *Inorg. Chem.*, 6 (12), 2250–2255, (1967).
- Pan, B.; Evers-McGregor, D.A.; Bezpalko, M.W.; Foxman, B.M.; Thomas, C.M.; Multimetallic Complexes Featuring a Bridging N-heterocyclic Phosphido/Phosphenium Ligand: Synthesis, Structure, and Theoretical Investigation, *Inorg. Chem.*, 52 (16), 9583–9589, (2013).
- Purgel, M.; Baranyai, Z.; Blas, A.; Rodriguez-Blas, T.; Bányai, I.; Platas-Iglesias, C.; Tóth, I.; An NMR and DFT Investigation on the Conformational Properties of Lanthanide(III) 1,4,7,10-Tetraazacyclododecane-1,4,7,10-tetraacetate Analogues Containing Methylene phosphonate Pendant Arms, *Inorg. Chem.*, 49 (9), 4370–4382, (2010).
- Hai-Sheng, R.; Mei-Jun, M.; Jian-Yi, M.; Xiang-Yuan, Li.; Theoretical Calculation of Reorganization Energy for Electron Self-Exchange Reaction by Constrained Density Functional Theory and Constrained Equilibrium Thermodynamics, *J. Phys. Chem. A*, 117 (33), 8017–8025, (2013).

- 12.- Caetano, M.S.; Ramalho, T.C.; Botrel, D.F.; da Cunha, E.F.F.; Mello, W.C.; Understanding the Inactivation Process of Organophosphorus Herbicides: A DFT Study of Glyphosate Metallic Complexes with Zn^{2+} , Ca^{2+} , Mg^{2+} , Cu^{2+} , Co^{3+} , Fe^{3+} , Cr^{3+} , and Al^{3+} , *International Journal of Quantum Chemistry*, 112, 2752–2762, (2012).
- 13.- Koo, I.N.; Ali, D.; Yang, K.; Park, Y.; Wardlaw, D.M.; Buncel, E.; Theoretical Study of ^{31}P NMR Chemical Shifts for Organophosphorus Esters, Their Anions and O,O-Dimethylthiophosphorate Anion with Metal Complexes, *Bull. Korean Chem. Soc.*, 29, 11, 2252-2258, (2008).
- 14.- Amsterdam Density Functional (ADF) Code, Release, Vrije Universiteit, Amsterdam, The Netherlands, 2007.
- 15.- E. Van Lenthe, E.J. Baerends, G. Snijders, Relativistic total energy using regular approximations, *J. Chem. Phys.*, 101, 9783, (1994).
- 16.- G. Te Velde, F.M. Bickelhaupt, S.J.A. Van Gisbergen, C. Fonseca Guerra, E.J. Baerends, J.G. Snijders, Chemistry with ADF, T.J. Ziegler, *Comput. Chem.*, 22, 931, (2001).
- 17.- L. Verluise, T. Ziegler, The determination of molecular structures by density functional theory. The evaluation of analytical energy gradients by numerical integration, *J. Chem. Phys.*, 88, 322, (1988).
- 18.- S.H. Vosko, L. Wilk, M. Nusair, Accurate spin-dependent electron liquid correlation energies for local spin density calculations: A critical analysis, *Can. J. Phys.*, 58, 1200, (1980).
- 19.- P.R.T. Schipper, O.V. Gritsenko, S.J.A. van Gisbergen, E.J. Baerends, Molecular calculations of excitation energies and (hyper)polarizabilities with a statistical average of orbital model exchange-correlation potentials, *J. Chem. Phys.*, 112, 1344, (2000).
- 20.- E. Runge, E.K.U. Gross, Density-Functional Theory for Time-Dependent Systems, *Phys. Rev. Lett.*, 52, 997, (1984).
- 21.- F. Wang, T. Ziegler, E. van Lenthe, S. van Gisbergen, E.J. Baerends, The calculation of excitation energies based on the relativistic two-component zeroth-order regular approximation and time-dependent density-functional with full use of symmetry, *J. Chem. Phys.*, 122, 204103, (2005).
- 22.- A. Klamt, V. Jonas, A Conductor-like screening model for real solvents: A new approach to the quantitative calculation of solvation phenomena, *J. Chem. Phys.*, 105, 9972, (1996).
- 23.- A. Klamt, Treatment of the outlying charge in continuum solvation models, *J. Phys. Chem.*, 99, 2224, (1995).
- 24.- N.M. O'Boyle, A.L. Tenderholt, K.M. Langner, CcLib: A library for package-independent computational chemistry algorithms, *J. Comput. Chem.*, 29, 839, (2008).
- 25.- Anita Drozd, Martina Bubrin, Jan Fiedler, Stanislav Z'ali's and Wolfgang Kaim, (a-Diimine)tricarbonylhalorhenium complexes: the oxidation side, *Dalton Trans.*, 41, 1013, (2012).
- 26.- F. H. Allen, O. Kennard, D. G. Watson, L. Brammer, A. G. Orpen. Tables of bond Lengths determined by X-Ray and Neutron Diffraction. Part 1. Bond Lengths in Organic Compounds. *J. Chem. Soc. Perkin Trans. II*, S1-S19, (1987).
- 27.- Andrzej Okuniewski and Barbara Becker, Ammonium O,O-diethyl dithiophosphate, *Acta Cryst.*, E67, o1749–o1750, (2011).
- 28.- Rindorf, G.; Carlsen, L. *Acta Cryst.*, B35, 1179, (1979).
- 29.- Kenneth B. Wiberg and Yigui Wang, A comparison of some properties of C=O and C=S bonds, *ARKIVOC* 2011 (v) 45-56.
- 30.- Athanassios C. Tsipis, Exploring the Forces That Control the P-C Bond Length in Phosphamides and Their Complexes: The Key Role of Hyperconjugation, *Organometallics*, 25, 2774-2781, (2006).
- 31.- Srinivasan Priya, Maravanji S. Balakrishna, Joel T. Mague, Shaikh M. Mobin, Insertion of Carbon Fragments into P(III)-N Bonds in Aminophosphines and Aminobis(phosphines): Synthesis, Reactivity, and Coordination Chemistry of Resulting Phosphine Oxide Derivatives. Crystal and Molecular Structures of $(Ph_2P(O)CH_2)_2NR$ ($R = Me, nPr, nBu$), $Ph_2P(O)CH(OH)nPr$, and *cis*- $[MoO_2Cl_2\{(Ph_2P(O)CH_2)_2NEt-KO, KO\}]$, *Inorganic Chemistry*, 42, 1272-1281, (2003).
- 32.- Sebastian Burck, Dietrich Gudat, Kalle Näntinen, Martin Nieger, Mark Niemeyer, Dirk Schmid, 2-Chloro-1,3,2-diazaphospholenes – A Crystal Structural Study, *Eur. J. Inorg. Chem.*, 5112–5119, (2007).
- 33.- Christoph E. Strasser, Stephanie Cronje and Helgard G. Raubenheimer, *Acta Cryst.*, E65, m86. doi:10.1107/S1600536808041809, (2009).
- 34.- Yan-Fei Zhang, Pei-Hua Zhao, Jun-Jie Liu and Gui-Zhe Zhao, *Acta Cryst.*, E67, o2861. doi:10.1107/S160053681104030X, (2011).
- 35.- R. Mattern and L. Nieland, *Inorganica Chimica Acta*, 112, 215-217, (1986).
- 36.- Stewart W. Bartlett, Simon J. Coles, David B. Davies, Michael B. Hursthouse, Hanife I. bis, og'lu, Adem Kilic, Robert A. Shawb and I. lker U'nc, *Acta Cryst.*, B62, 321–329. doi:10.1107/S0108768106000851, (2006).
- 37.- C. Akers, S.W. Peterson and R. D. Willett, *Acta Cryst.*, B24, 1125, (1968).
- 38.- Reeve, R. N. Aspects of the coordination chemistry of phosphorus(V) chloro-compounds, Durham theses, Durham University, 1975.
- 39.- George Socrates, *Infrared and Raman Characteristic Group Frequencies: Tables and Charts*, 3th ed.; John Wiley & Sons, Ltd: Chichester, England, , p. 82-90, 2001.
- 40.- (Shaoyi Jiang, Siddharth Dasgupta, Mario Blanco, Rawls Frazier, Elaine S. Yamaguchi, Yongchun Tang,) and William A. Goddard, ,†Structures, Vibrations, and Force Fields of Dithiophosphate Wear Inhibitors from *ab Initio* Quantum Chemistry, *J. Phys. Chem.*, 100, 15760-15769, (1996).
- 41.- D. H. Boal, G. A. Ozin, Studies of some thermally unstable complexes of group V trihalides with trimethylamine and $[^2H_3]$ trimethylamine by infrared, Raman, and matrix-isolation Raman spectroscopy, normal coordinate analysis, and structural methods, *J. Chem. Soc., Dalton Trans.*, 1824-1828, (1972).
- 42.- Hajar Sahebalzamani, Shahriare Ghammamy, Kheyrollah Mehrani, Shahram Jahandide, Farshid Salimi, Density functional theory studies of structural properties, energies and natural band orbital for two new aluminate compounds, *Spectrochimica Acta Part A* 90, 218– 222, (2012).
- 43.- K.A.E. Roberts, Neil J. Brown, Hannah N. Roberts, Joseph J.W. McDouall, Paul J. Low, Mark W. Whiteley, Electronic structure and spectroscopy of the cycloheptatrienyl molybdenum halide complexes $[MoBrL_2(g-C_7H_7)]^{n+}$ ($L_2 = 2CO, n = 0; L_2 = 2,20$ -bipyridyl, $n = 0$ or 1), *Polyhedron*, in press (2014)
- 44.- Reshak, A. H, Sikander Azam., “Theoretical Study Of The Structural, Electronic Structure, Fermi Surface, Electronic Charge Density and Optical Properties of the of $LnVO_4$ ($Ln = Sm, Eu, Gd$ and Dy)” *Int. J. Electrochem. Sci.*, 8, 10396 – 10423, (2013).
- 45.- P.P. Moorthi, S. Gunasekaran, S. Swaminathan, G.R. Ramkumaar, Quantum chemical density functional theory studies on the molecular structure and vibrational spectra of mannitol, *Spectrochimica Acta Part A: Molecular and Biomolecular Spectroscopy*, 137, 412–422, (2015).
- 46.- Jursic, B.S. “A B3LYP hybrid density functional theory study of structural properties, energies, and heats of formation for silicon–hydroge compounds” *Journal of Molecular Structure (Theochem)* 497, 65–73, (2000).
- 47.- V. Nagarajan, R. Chandiramouli, TeO_2 nanostructures as a NO_2 sensor: DFT investigation, *Computational and Theoretical Chemistry*. 1049, 20–27, (2014).

ACKNOWLEDGMENTS

We gratefully acknowledge the financial support of the Research Council of Imam Khomeini International University. RRT gratefully acknowledges the financial support of Fondecyt 1130007. Acknowledge the financial support of DIN 02/2013 UCSC.